



# *Buchholzia coriacea* Leaves Attenuated Dyslipidemia and Oxidative Stress in Hyperlipidemic Rats and Its Potential Targets *In Silico*

Daniel E. Uti<sup>1\*</sup> Udu A. Ibiam<sup>2,3</sup> Wilson A. Omang<sup>4</sup> Precious A. Udeozor<sup>3</sup> Grace U. Umoru<sup>3</sup>  
Solomon K. Nwadam<sup>5</sup> Inalegwu Bawa<sup>1</sup> Esther U. Alum<sup>2</sup> Joseph C. Mordi<sup>6</sup> Edith O. Okoro<sup>7</sup>  
Uket Nta Obeten<sup>8</sup> Eucharia N. Onwe<sup>9</sup> Suleiman Zakari<sup>1,10</sup> Ohunene Rukayat Opotu<sup>2</sup> Patrick M. Aja<sup>2</sup>

<sup>1</sup> Department of Biochemistry, Faculty of Basic Medical Sciences, College of Medicine, Federal University of Health Sciences, Otuokpo, Benue State, Nigeria

<sup>2</sup> Department of Biochemistry, Faculty of Science, Ebonyi State University, Abakaliki, Ebonyi State, Nigeria

<sup>3</sup> Department of Biochemistry, College of Science, Evangel University Akaeze, Abakaliki, Ebonyi State, Nigeria

<sup>4</sup> Department of Medical Laboratory Technology, Cross River State College of Health Technology, Calabar, Nigeria

<sup>5</sup> Department of Pharmacology and Therapeutics, Faculty of Clinical Basic Medicine, Ebonyi State University, Abakaliki, Nigeria

<sup>6</sup> Department of Medical Biochemistry, Delta State University, Abraka, Nigeria

<sup>7</sup> Department of Medical Laboratory Science, Delta State University, Abraka, Nigeria

**Address for correspondence** Daniel E. Uti, PhD, Department of Biochemistry, Faculty of Basic Medical Sciences, College of Medicine, Federal University of Health Sciences, Akwete-Akpa 972224, Benue State, Nigeria

(e-mail: daniel.uti@fuhso.edu.ng; dan4uti@gmail.com).

<sup>8</sup> Department of Chemistry/Biochemistry and Molecular Biology, Alex Ekwueme Federal University, Ndufu-Alike Ikwo, Abakaliki, Ebonyi State, Nigeria

<sup>9</sup> Department of Biotechnology, College of Science, Evangel University, Akaeze, Ebonyi State, Nigeria

<sup>10</sup> CAPlGACE Cancer Research Group, Department of Biochemistry, Covenant University, Ota, Ogun State, Nigeria

Pharmaceut Fronts 2023;5:e141–e152.

## Abstract

The study aimed to investigate how the solvent extract of *Buchholzia coriacea* (BCE), a widely known hypolipidemic agent, could contribute to hyperlipidemia treatment and identify the potential bioactive compounds. We studied Wistar albino rats, dividing them into seven groups: the normal control, normal rats treated with 400 mg/kg.b.wt of BCE (NRG group), the hyperlipidemic control (HPC group), hyperlipidemic rats treated with atorvastatin, a standard control drug (SC group), as well as 200, 400, and 800 mg/kg.b.wt of BCE extract respectively (T1, T2, T3 groups). The potential compounds that functioned in BCE extract were analyzed by *in silico* binding to acetyl-CoA carboxylase (ACC) and fatty acid synthase (FASN). The binding affinities and drug-like properties of the compounds were determined using virtual screening and absorption distribution metabolism excretion and toxicity prediction analysis. The gas chromatography-mass spectrometry analysis identified alkaloids, saponins, flavonoids, phenols, terpenoids, and 44 chemical compounds in the leaf extract of BCE. BCE significantly reduced the levels of triacylglycerol, total cholesterol, low-density lipoprotein, very low-density lipoprotein, atherogenic coefficient, atherogenic index, and coronary risk index, while enhancing the levels of high-density lipoprotein and cardioprotective index in comparison to the HPC group. The BCE reduced

## Keywords

- ▶ *Buchholzia coriacea*
- ▶ lupenone
- ▶ 2,7-dimethylnaphthalene
- ▶ acetyl-CoA carboxylase
- ▶ fatty acid synthase
- ▶ hyperlipidemia

received

March 3, 2023

accepted

July 26, 2023

article published online

September 5, 2023

DOI <https://doi.org/>

10.1055/s-0043-1772607.

ISSN 2628-5088.

© 2023. The Author(s).

This is an open access article published by Thieme under the terms of the Creative Commons Attribution License, permitting unrestricted use, distribution, and reproduction so long as the original work is properly cited. (<https://creativecommons.org/licenses/by/4.0/>)

Georg Thieme Verlag KG, Rüdigerstraße 14, 70469 Stuttgart, Germany

malondialdehyde quantities, which exhibit high levels in HPC. Superoxide dismutase and glutathione peroxidase activities as well as glutathione levels, which are otherwise reduced in HPC, were increased upon the BCE treatment. Among the identified BCE compounds, lupenone and 2,7-dimethylnaphthalene exhibited the highest binding affinities to ACC and FASN, suggesting that these two compounds might be the bioactive BCE components displaying hypolipidemic properties. BCE is found to be beneficial in blocking hyperlipidemia through the modulation of lipid profile, the protection of cardiovascular function, as well as the suppression of oxidative stress. BCE may be a natural source for exploring novel drugs for the treatment of dyslipidemia.

## Introduction

There is an increasing reliance on medicinal plants in the case of various disease treatments both in Africa and worldwide,<sup>1</sup> due to ingested chemical deposits that might exhibit therapeutic benefits. Managing the cholesterol, especially low-density lipoprotein cholesterol (LDL-c), levels in the body is reportedly crucial to prevent cardiovascular disease-associated conditions.<sup>2,3</sup>

Acetyl-coenzyme A (acetyl-CoA) is a rate-limiting enzyme in fatty acid metabolism.<sup>4</sup> Malonyl-CoA, the product of acetyl-CoA carboxylase (ACC) catalysis, is essential for triggering fatty acid synthase spiral reactions, another essential enzyme for lipid biosynthesis.<sup>5</sup> Abnormal fatty acid metabolism due to increased fatty acid synthesis by the fatty acid synthase activities initiated by the ACC activities is a hallmark of glycolipid metabolic diseases.<sup>6</sup> Therefore, the inhibitors of these enzymes were the focus of the preceding search for therapies against various human diseases such as diabetes mellitus, cancer, obesity, and metabolic syndrome, aiming at the prevention of hyperlipidemia (i.e., increased blood lipid levels). As cells use glucose, pyruvate is the end product of the first process of glucose metabolism, known as the glycolytic pathway. Pyruvate undergoes decarboxylation in the mitochondria by an intermediate acetyl-CoA, then it becomes the substrate for the next step in the energy cycle, the tricarboxylic acid cycle, supplying a certain amount of adenosine triphosphate (ATP).<sup>5</sup> The product ACC, along with malonyl-CoA, serves as a substrate for fatty acid synthase (FASN), an enzyme responsible for the biosynthetic process catalysis of the FASN spiral, in a nicotinamide-adenine-dinucleotide-phosphate-reduced (NADPH)-dependent reaction.

Years of research effort in natural products, chemistry, and biochemistry resulted in advances in the design and discovery of numerous inhibitors of these enzymes. *Buchholzia coriacea* (BCE) is a forest tree of the Capparaceae family.<sup>7</sup> An earlier study revealed that the anti-inflammatory, antiulcer, antihelmintic, anti-inflammatory, antioxidant, antihyperlipidemic, antihypercholesterolemic, antiatherogenic, antitrypanosomal, antimodulatory, antispasmodic, antidiarrhea, and antifertility BCE plant properties have been scientifically validated.<sup>7</sup> These BCE properties endowed this plant with significant advantages as a medicinal plant compared with other plants of the same class. Therefore,

research into BCE and its derivatives as a natural plant source is necessary, as it could represent a further alternative in the search for hypolipidemic agents in the treatment of dyslipidemia.

Moreover, the seeds of the plant are edible with a peppery taste and are known for their high medicinal value, giving the plant its common name, wonderful kola.<sup>7</sup> This plant has been used to treat various diseases in different parts of Africa over the years. Recent studies of this plant's seed extract demonstrated that it is a good source of energy and possesses antibacterial, antidiabetic, hypolipidemic, antioxidant, and antiulcer activities.<sup>8</sup> This study thus aimed at investigating the hypolipidemic potential of BCE both *in vivo* and *in silico* against ACC and FASN, key proteins that are involved in the lipogenesis pathway, potentially providing opportunities to search for therapies against hyperlipidemia and associated disease complications.

## Materials and Methods

### Plant Collection

BCE plants were obtained from a farm in Abakaliki, Ebonyi State, Nigeria, and taken to Evangel University Biochemistry Laboratory for authentication by Dr. Bruno Ado at the Biology Division, Department of Biotechnology, then dried at room temperature between 23°C and 25°C.

### Crude Extract Preparation

The leaves were cut into pieces and dried at room temperature (25–29°C). The dried leaves were ground and soaked in methanol at a sample-to-solvent ratio of 1:3. The suspension was stirred in an electric mixer and left to stand for approximately 48 hours at room temperature, then filtered.<sup>9</sup> The filtrate was then concentrated as described previously.<sup>10</sup>

### Phytochemical Plant Extract Screening

To conduct both qualitative and quantitative phytochemical analyses for identifying the components present in the plant extract, standard procedures were used as described previously.<sup>11–13</sup> Briefly, when testing for alkaloids, 0.1 g of the extract was supplemented with 10 mL of acidified alcohol, the mixture was then heated and filtered to investigate the potential alkaloid content. Next, 1 mL of filtrate was supplemented with 0.4 mL of diluted ammonia and 1 mL of

chloroform, then the solution was gently shaken. The chloroform layer was extracted using 2 mL of acetic acid, then separated into two sections, with one being supplemented with Mayer's and the other with Dragendorff's reagent. For the alkaloid test, the appearance of a cream (when using Mayer's reagent) or a reddish-brown precipitate (when using Dragendorff's reagent) was considered positive. When testing for saponins, the production of an emulsion after adding three drops of olive oil to the froth created by mixing 0.1 g of extract with 1 mL of distilled water indicated saponin presence. To detect flavonoids, we performed an alkaline reagent test. The presence of flavonoids was indicated by the test solution developing a strong yellow color following its supplementation with a few drops of sodium hydroxide solution, which turns colorless upon the addition of a few drops of diluted acid. Using Salkowski's test, terpenoids were identified when strong sulfuric acid and 0.4 mL of chloroform were added to 0.1 g of extract, and a reddish-brown coloring formed on the interface, indicating terpenoid presence. When 50 mg of the extract was dissolved in 5 mL of distilled water and a few drops of a neutral 5% ferric chloride solution were added to it, the development of a dark green hue was considered a sign of phenolic compound presence. Using established techniques, the quantitative phytochemical screening was completed as previously reported.<sup>11–13</sup>

### Gas Chromatography-Mass Spectrometry Analysis of the Extracts

Batch processing of the solvent-extracted sample was used in the process of sample preparation of gas chromatography-mass spectrometry (GC-MS). Therefore, the chemicals were efficiently extracted from the sample within less time. The components of the sample were separated using the stationary phases of 5% diphenyl-95% dimethyl polysiloxane before loading. The chemical composition of the extract was then analyzed using the Agilent GC-MS (Model No. 19091S-933) equipped with an HP-1 millisecond capillary column (0.25 mm id. × 30 m specification length × 0.25 mL film thickness) and an autosampler as described previously.<sup>14</sup> Briefly, the conditions were maintained as follows: initial temperature and time, 70°C for 2 minutes, then raised to 350°C at a rate of 20°C/min and maintained for 20 minutes; 350°C for MSD transfer line heater; the carrier gas was helium at a flow rate, split ratio, and run time of 1.2 mL/min, 10:1, and 32.50 minutes, respectively.

### Animals

We used 42 healthy adult male albino rats in this study, purchased from the farm of Daniel Okoro in Abakaliki, Ebonyi State, Nigeria. The animals were given a week to get used to the laboratory environment before the start of the experiment. The animals were kept in cages and given a regular pellet as diet and water ad libitum.

### Experimental Design

A total of 42 male albino rats, weighing between 150 and 180 g, were divided into seven experimental groups ( $n = 6$ ). Hyperlipidemia induction in rats was established by three

intraperitoneal administrations of poloxamer P-407 (BASF Corporation; Mount Olive, New Jersey, United States) as follows: initial induction at 1g/kg.b.wt and two additional doses (one at 0.5 g/kg of P-407 on day 7 and another on day 11 following the initial induction) for maintaining hyperlipidemia.<sup>15</sup> Hyperlipidemia was confirmed 48 hours after the first hyperlipidemic induction. Blood was collected via cardiac puncture and used to ascertain the hyperlipidemic state of the rats using a Cardio Check device (Mission Cholesterol Meter, model number: CCM-111, Germany). Atorvastatin (Ceno Pharmacy Ltd., Ebonyi State, Nigeria) was used as the reference drug. Normal rats were treated with 0.5 mL normal saline (the normal control [NC] group) and 400 mg/kg.b.wt BCE (the normal rats treated [NRT] group). Hyperlipidemic rats were treated with 0.5 mL normal saline (the HPC group), 10 mg/kg.b.wt. atorvastatin (the standard control [SC] group), as well as 200, 400, and 800 mg/kg.b.wt of BCE (hyperlipidemic treated groups 1, 2, and 3 [T1, T2, and T3]), administered orally as earlier used daily for 21 days.<sup>16</sup> The treatment started 48 hours after the initial induction and immediately upon the confirmation of the hyperlipidemic state, while lower doses of P-407 (0.5 g/kg.b.wt) for hyperlipidemia maintenance were repeated on days 7 and 11 following the initial induction) as earlier used.<sup>15</sup> The animals in all groups were allowed free access to feed and water and the treatment lasted for 21 days, then the animals were sacrificed under chloroform inhalation anesthesia and the samples were obtained. Biochemical testing was then performed on the recovered supernatant (serum). This study was approved both by the Institutional Ethical Committee on Animal Rights and the Department of Biochemistry Ethical Committee on Research and Innovation (FUHSO/ET/BCH/22/002).

### Biochemical Parameter Determination

#### Serum Lipid Determination

Spectrophotometric techniques were used to measure the serum level of total cholesterol (TC), as explained by a reported study.<sup>17</sup> The level of serum triacylglycerols (TAG) was assessed using the Randox kit (Randox Laboratories Limited, United Kingdom).<sup>18</sup> Serum level of high-density lipoprotein cholesterol (HDL-C) was measured by the Warnick and colleague's method.<sup>19</sup> The following equation was used to determine the serum level of LDL-C following Friedewald et al's protocol<sup>20</sup>:  $TG/5 - HDL - c = LDL - c$  (mg/dL). The value was given in milligrams per deciliter. The formulas for calculating the atherogenic coefficient (AC), atherogenic index (AI), and coronary risk index (CRI) were as previously described:  $AC = [TC - HDL - C / HDL - C]$ ,  $AI = \text{Log}[TG / HDL - C]$ , and  $CRI = [TC / HDL - C]$ , respectively. The assessment of the cardioprotective index (CPI) was based on the HDL-C/LDL-C ratio.<sup>21</sup>

#### Oxidative Stress Indicator Evaluation

Thiobarbituric acid reactive substances (TBARS) were measured as lipid peroxidation markers using the Buege and Aust's technique.<sup>22</sup> The following antioxidant activity tests

were performed. Superoxide dismutase (SOD) was measured using a previously described technique for SOD activity determination.<sup>23</sup> The reduced glutathione test (GSH) procedure was based on the concept first proposed by Ellman<sup>24</sup> in 1959 and revised by Hu in 1994.<sup>25</sup> The technique we applied to assess glutathione peroxidase (GPX) activity was the one Hu and Ellman adapted and described in the assessment of sulfhydryl groups.<sup>24</sup>

### In Silico Studies

#### Target Preparation

The ACC (PDB-ID: 1UYS) and FASN (PDB-ID: 2PX6) structures were extracted from the Protein Data Bank (PDB) structure database (<https://www.rcsb.org/>). An open-source molecular editor was used to import the structures (Discovery Studio Visualizer 4.0). The structures were saved in PDB format after co-crystal ligand and heteroatom removal. Chimera UCSF was used to optimize the structure, consisting of 1,000 steps of the steepest descent followed by 1,000 steps of the conjugate gradient of the energy minimization method. The ligands were accessed from the PubChem database (<https://pubchem.ncbi.nlm.nih.gov/>), then their structures were loaded into the DS-Visualizer and saved as PDB files. We performed the virtual screening of 46 compounds based on the binding energy scores with targeted macromolecules ACC (1UYS) and FASN (2PX6) using the PyRx software.<sup>26</sup> Among the 46 ligands, we discovered that lupenone (92158) and 2,7-dimethylnaphthalene (11396) displayed the maximum dock scores. ACC (1UYS)-lupenone and FASN (2PX6)-2,7-dimethylnaphthalene displayed binding affinity ratings of  $-8.8$  and  $-7.7$ , respectively. Based on the binding affinities, two ligands were selected for verification using the AutoDock MGL tool 1.5.6. From each ligand, the nine best-docked poses with the highest to lowest binding energies were obtained, out of which the best-docked pose with the highest binding energies was considered for redocking and further analysis.

#### Molecular Docking Studies

The receptor protein for docking was produced in the AutoDock format.<sup>27</sup> To construct the receptor lattice, we used

residues around 1 of 1UYS and 2PX6 associated with the co-crystal of lupenone and 2,7-dimethylnaphthalene. Receptors and ligands were saved in a pdbqt format for later use with the MGL program. Vina was started from a command prompt on the command line. In the setup, the standard grid spacing was 0.425 and the completeness was set to 8. The output files were in a pdbqt format and were submitted for analysis with PyMol and the Discovery Studio Visualizer 2021. The 1UYS and 2PX6 structures were reduced using the steepest descent method (1,000 steps) followed by the inclusion of the AMBER ff4 force field before the docking research was performed with the relevant ligands. Before the interaction studies, the protonation states of the 1UYS and 2PX6 involved were tested for neutralization. Autodocking v 4.2.6 was used to perform the molecular docking experiments. Both the receptor and the ligands were created by combining polar hydrogen bonds with Kollman and Gasteiger charges. Finally, both receptor and ligand molecules were saved in a pdbqt format after the nonpolar hydrogen atoms were combined. A mesh box was produced with the values as follows:  $X = 20$ ,  $Y = 18$ , and  $Z = 32$  with a distance of 0.3. The protein–ligand complex docking experiments were performed with the Lamarckian Genetic Algorithm to obtain the lowest free energy of binding (G).

#### Lupenone Lead Optimization

The most pronounced concern for the pharmaceutical industry in new drug molecule detection and development is the expected bioavailability, which is influenced by solubility.<sup>28</sup> In this study, though lupenone exhibited strong ACC binding and inhibition potentials, representing a strong new drug development candidate for dyslipidemia management, the carbon skeleton of this compound presented a major concern in the future drug development process due to its low solubility features and complex carbon structure. Hence, lupenone (**Fig. 1A**) was optimized to a better lupenone derivative (**Fig. 1B**) using the ADMETopt web server.<sup>29</sup> **Fig. 1C, D** presents the optimized molecules (I, II, and III) and 2,7-dimethylnaphthalene, respectively. In this case “III” was used for further docking in the AutoDock MGL tool 1.5.6 with the ACC (1UYS). The lupenone derivative was drawn using the software Marvin Sketch from the Chemaxon

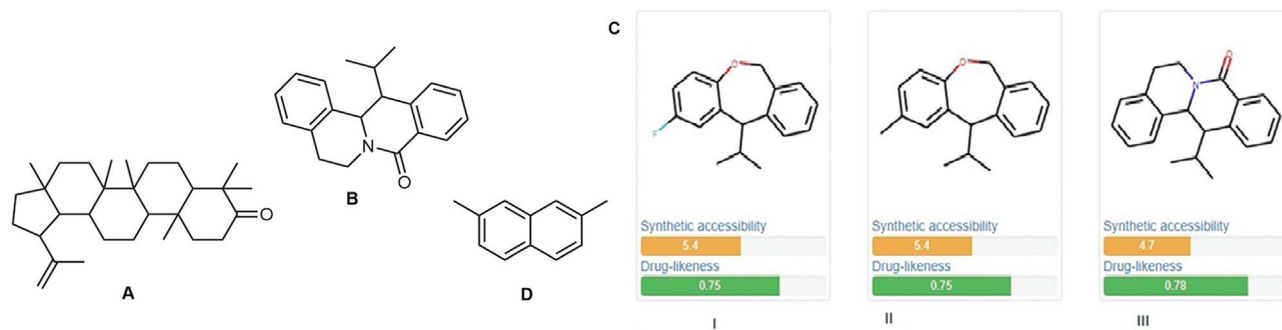


**Fig. 1** The structures of top-posed compounds and their optimized derivatives. (A) Lupenone; (B) optimized lupenone; (C) optimized lupenone molecules using ADMETopt server, indicating their drug-likeness and synthetic accessibility; (D) 2,7-dimethylnaphthalene structure.

web server (<https://chemaxon.com/products/marvin>) and saved in a PDB format before docking preparation.

### Absorption Distribution Metabolism Excretion and Toxicity/Pharmacokinetics Prediction Analysis of Top-Posed Compounds

The absorption distribution metabolism excretion and toxicity (ADMET)/pharmacokinetics prediction analysis of the top-posed compounds was performed using the online web servers SwissADME (<http://www.swissadme.ch/>)<sup>30</sup> and admetSAR (<http://lmmd.ecust.edu.cn>). This Web site allows for calculating physicochemical descriptors and predicting ADME parameters, pharmacokinetic properties, drug-like nature, and medicinal chemistry friendliness of one or more small molecules in the drug discovery process using the canonical Simplified Molecular Input Line Entry Specification of the investigated compounds or potential drugs.

### Statistical Analysis

The differences between the treated and control groups were statistically evaluated using a one-way analysis of variance coupled with a one-sample *t*-test. The results were expressed as the mean ± standard deviation. GraphPad Prism7 was used to complete all statistical calculations. *p*-Values of <0.05 were considered statistically significant.

## Results

### Qualitative and Quantitative Phytochemical BCE Composition

The qualitative BCE leaf extract analysis indicated the presence of tannins, flavonoids, terpenoids, alkaloids, saponins, and phenols, while steroids, cardiac glycosides, and reducing sugars were not in a detectable amount (►Table 1). ►Fig. 2 depicts the quantitative analysis of phytochemical constituents, indicating a high-level presence of flavonoids with a significant presence of saponins, alkaloids, terpenoids, phenols, and tannins.

### GC-MS-Detected Methanolic BCE Extract Chemical Profiles

The chemical composition of the extract was analyzed using Agilent GC-MS (►Table 2). We detected 44 chemical compounds from the plant using the GC-MS technique, which we summarized here indicating the PubChem ID, molecular formula, and chemical quality.

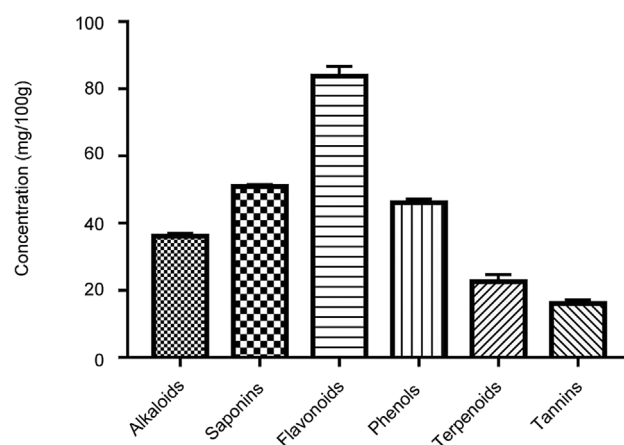


Fig. 2 Phytochemical composition of BCE. BCE, *Buchholzia coriacea*.

### Extract Treatment Effects on Lipid Profiles in P-407-Induced Hyperlipidemic Rats

►Fig. 3 presents treatment effects on P407-induced hyperlipidemic rats. Our data showed that the TAG level was significantly increased in the HPC group ( $p < 0.05$ ) compared with the NC; however, the treatment groups (SC, NRT, and T1–T3) significantly reduced TAG levels to those similar to NC. Similar observations were seen in TC, LDL, and very low-density lipoprotein (VLDL) in different groups. However, a reciprocal effect could be observed on serum HDL concentration, where reduced HDL in HPC compared with NC was increased upon the various treatments (SC, NRT, and T1–T3).

### Treatment Effect on Cardiovascular Function Indices

Next, we assessed the effect of leaf extracts on expression levels of cardiovascular functional markers (AC, AI, CRI, and CPI). As shown in ►Fig. 4, in comparison to atorvastatin, the gold standard medication, a high dose of BCE was more effective at defending the rats against cardiovascular risk markers. AC, AI, and CRI were significantly enhanced in the HPC group, and the changing trend was significantly reversed by additional treatment (SC, NRT, T1–T3). CPI levels, significantly reduced in the HPC group, was markedly increased upon different treatment (SC, NRT, T1–T3) ( $p < 0.05$ ).

### Treatment Effect on Lipid Peroxidation and Oxidative Stress Markers

The lipid peroxidation marker TBARS-malondialdehyde (MDA) levels in the HPC group significantly ( $p < 0.05$ ) increased, and with additional treatment of leaf-extracts

Table 1 Results of phytochemical screening for *Buchholzia coriacea*

	Tannin	Flavonoid	Terpenoid	Alkaloid	Saponin	Steroid	Cardiac glycoside	Reducing sugar	Phenol
Extracts of <i>Buchholzia coriacea</i>	+	+	+	+	+	–	–	–	+

Note: +: present; –: not detected.

**Table 2** Chemical profile of *Buchholzia coriacea*; obtained from gas chromatography-mass spectrometry analysis

SN	RT	TC (%)	Library ID (Nistill)	PubChem Id	Molecular formula	Quality
1	5.600	0.11	2,3-Dihydrobenzofuran	10329	C <sub>8</sub> H <sub>8</sub> O	72
2	5.686	0.15	2-Methylbenzaldehyde	10722	C <sub>8</sub> H <sub>8</sub> O	81
3	5.915	0.13	2-Cyclohexen-1-one, 2-hydroxy-6-methyl-3-(1-methylethyl)-	108261	C <sub>10</sub> H <sub>16</sub> O <sub>2</sub>	46
4	6.744	0.25	2-Methoxybenzoic acid	11370	C <sub>8</sub> H <sub>8</sub> O <sub>3</sub>	81
5	6.973	0.24	2,7-Dimethylnaphthalene	11396	C <sub>12</sub> H <sub>12</sub>	27
6	7.202	0.41	4H-Pyran-4-one, 2,3-dihydro-3,5-dihydroxy-6-methyl-	119838	C <sub>6</sub> H <sub>8</sub> O <sub>4</sub>	14
7	7.568	0.30	Butyl ethyl ether	12355	C <sub>6</sub> H <sub>14</sub> O	47
8	7.649	0.31	2,3,4,5-Tetrachloroanisole	13649	C <sub>7</sub> H <sub>4</sub> Cl <sub>4</sub> O	50
9	8.015	0.25	2,5-Cyclohexadienylbenzene	20927	C <sub>12</sub> H <sub>12</sub>	38
10	7.649	0.31	Benzoic acid	243	C <sub>6</sub> H <sub>5</sub> COOH	50
11	8.118	0.33	Benzyl alcohol	244	C <sub>6</sub> H <sub>5</sub> CH <sub>2</sub> OH	95
12	8.272	0.41	2(1H)-Naphthalenone, 1-(acetyloxy)octahydro-4a,8a-dimethyl-	278215	C <sub>14</sub> H <sub>22</sub> O <sub>3</sub>	76
13	8.541	0.21	Palmitoleic acid	445638	C <sub>16</sub> H <sub>30</sub> O <sub>2</sub>	43
14	8.684	0.12	2-Methoxy-4-vinylphenol	332	C <sub>9</sub> H <sub>10</sub> O <sub>2</sub>	15
15	9.159	0.27	2,6,10-Dodecatrien-1-ol, 3,7,11-trimethyl-	3327	C <sub>15</sub> H <sub>26</sub> O	49
16	9.279	0.37	2(1H)-Naphthalenone, octahydro-4a-methyl-7-(1-methylethyl)-	41133	C <sub>14</sub> H <sub>24</sub> O	87
17	10.080	0.23	Palmitoleic acid	445638	C <sub>16</sub> H <sub>30</sub> O <sub>2</sub>	46
18	10.183	0.08	Oleic acid	445639	C <sub>18</sub> H <sub>34</sub> O <sub>2</sub>	86
19	10.326	0.16	2-Hexenoic acid	5282707	C <sub>6</sub> H <sub>10</sub> O <sub>2</sub>	84
20	10.498	0.30	3-Hexenoic acid	5282708	C <sub>6</sub> H <sub>10</sub> O <sub>2</sub>	68
21	10.647	0.10	Oleamide	5283387	C <sub>18</sub> H <sub>35</sub> NO	42
22	10.727	0.51	cis-13-Octadecenoic acid	5312441	C <sub>18</sub> H <sub>34</sub> O <sub>2</sub>	99
23	10.797	0.27	Tris(aziridinomethyl)hydrazine	535658	C <sub>9</sub> H <sub>19</sub> N <sub>5</sub>	25
24	11.076	0.16	2-Butyl-2-octenal	5362697	C <sub>12</sub> H <sub>22</sub> O	52
25	11.162	0.29	(Z)-7-Hexadecenal	5364438	C <sub>16</sub> H <sub>30</sub> O	81
26	11.316	0.14	3-Methyl-4-(methoxycarbonyl)hexa-2,4-dienoic acid	5365038	C <sub>9</sub> H <sub>12</sub> O <sub>4</sub>	52
27	11.488	0.49	1H-Indene, 1-ethylidene-	5372637	C <sub>11</sub> H <sub>10</sub>	35
28	11.654	0.18	1-Bromo-11-iodoundecane	549994	C <sub>11</sub> H <sub>22</sub> BrI	49
29	11.763	0.13	1-[4-(Hydroxymethyl)phenyl]ethanol	578171	C <sub>9</sub> H <sub>12</sub> O <sub>2</sub>	50
30	12.054	0.30	Oxazole, 2,5-dimethyl-4-phenyl-	599323	C <sub>11</sub> H <sub>11</sub> NO	41
31	12.135	0.07	2-Benzofurancarboxaldehyde	61341	C <sub>9</sub> H <sub>6</sub> O <sub>2</sub>	18
32	12.220	0.14	Actinidiolide, dihydro-	6432173	C <sub>11</sub> H <sub>16</sub> O <sub>2</sub>	30
33	12.306	0.05	Ethanol, 2-(3,3-dimethylcyclohexylidene)-, (2E)-	6449789	C <sub>10</sub> H <sub>18</sub> O	64
34	12.398	0.46	3,4,5-Trimethoxyphenol	69505	C <sub>9</sub> H <sub>12</sub> O <sub>4</sub>	43
35	12.701	0.21	o-Toluidine	7242	C <sub>7</sub> H <sub>9</sub> N	46
36	12.827	0.76	Methyl 2,5-dihydroxybenzoate	75077	C <sub>8</sub> H <sub>8</sub> O <sub>4</sub>	93
37	13.119	0.59	4-Ethylcyclohexanone	79506	C <sub>8</sub> H <sub>14</sub> O	83
38	13.199	0.21	Benzyl salicylate	8363	C <sub>14</sub> H <sub>12</sub> O <sub>3</sub>	30
39	13.330	0.78	Citronellyl propionate	8834	C <sub>13</sub> H <sub>24</sub> O <sub>2</sub>	70
40	13.422	1.74	Ethyl hexopyranoside	91694274	C <sub>8</sub> H <sub>16</sub> O <sub>6</sub>	50

Table 2 (Continued)

SN	RT	TC (%)	Library ID (Nistill)	PubChem Id	Molecular formula	Quality
41	13.548	0.37	Lupenone	92158	C <sub>30</sub> H <sub>48</sub> O	89
42	13.594	0.74	Palmitic acid	985	C <sub>16</sub> H <sub>32</sub> O <sub>2</sub>	62
43	13.725	0.78	2-Propenal, 3-(4-hydroxy-3-methoxyphenyl)-	9984	C <sub>10</sub> H <sub>10</sub> O <sub>3</sub>	68
44	13.811	1.69	2-Phenylacetic acid	999	C <sub>8</sub> H <sub>8</sub> O <sub>2</sub>	81

Abbreviations: RT, retention time; TC, total concentration.

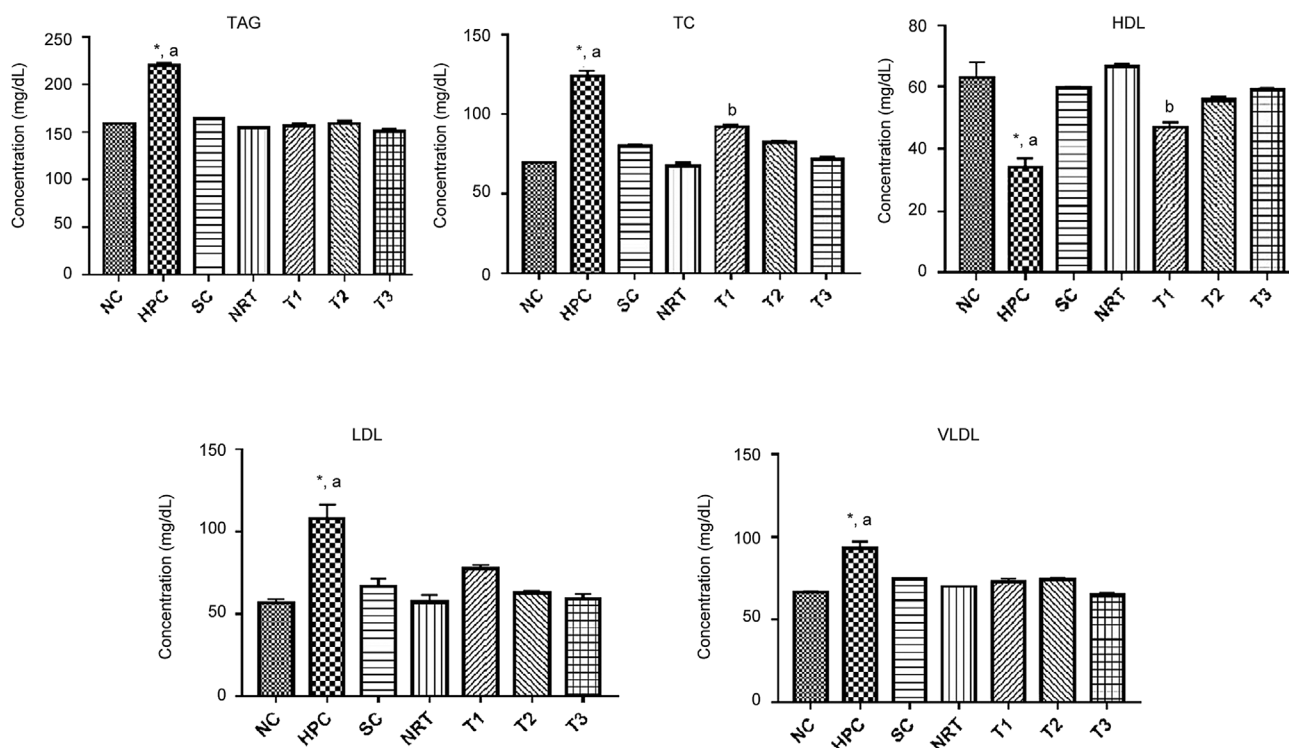


**Fig. 3** Effects of BCE extract on lipid profile of hyperlipidemic rats induced by poloxamer 407. \* $p < 0.05$  vs. NC; <sup>a</sup> $p < 0.05$  vs. the treatment groups (SC, NRT, T1, T2, T3); <sup>b</sup> $p < 0.05$  vs. T3. BCE, *Buchholzia coriacea*; HDL, high-density lipoprotein; LDL, low-density lipoprotein; TAG, triacylglycerol; TC, total cholesterol; VLDL, very low-density lipoprotein.

(T1–T3) and the standard drug (SC), the changing trend was significantly reversed ( $p < 0.05$ ) (►Fig. 5). Similarly, SOD and the activities of GPX and GSH were significantly decreased in HPC rats relative to NC rats (►Fig. 5,  $p < 0.05$ ). However, these SOD- and glutathione-related characteristics significantly and dose-dependently ( $p < 0.05$ ) increased following the leaf extract and standard drug treatments.

### Virtual Compound Screening

The ACC-lupenone and FASN-2,7-dimethylnaphthalene complexes (1UYS-92158 and 2PX6-11396, respectively) exhibited binding affinity scores of  $-8.8$  and  $-7.7$  binding affinity dock scores, which were better than those of the two standard inhibitors of these proteins (UYS-71528744 [firso-costat] with  $-6.7$  and 2PX6-9881506 [C75 trans] with  $-5.7$ ). These best two molecules were further re-docked at the 1UYS and 2PX6 binding cavities. Out of 46 ligands screened for both receptors, two ligands lupenone and 2,7-dimethyl

naphthalene (Chem ID: 92158 and 11396, respectively in ►Table S1 [Supporting Information]) with the Rmsd score 2.507 with 1UYS-92158 and Rmsd score 0.329 with 2PX6-11396 showed the lowest binding energies, suggesting the highest binding affinities. This binding energy-based virtual screening gave us a vivid idea of the best ligand with the highest affinity to ACC (1UYS) and FASN (2PX6). The 3D representation of these interactions are as shown in ►Fig. 6.

### Molecular Docking Studies

Molecular interaction in re-docking studies of the lupenone ligand with ACC (1UYS) highlighted a well-defined binding pocket constituted of leucine, proline, alanine, asparagine, tyrosine, leucine, and glutamine residues, where the ligand bound to the core of the pocket with a binding energy of ( $\Delta$ )  $-12$  kcal/mol and inhibitory concentration ( $K_i$ ) of  $1.59$   $\mu\text{mol/L}$ . Moreover, after re-docking with the 2,7-dimethylnaphthalene ligand with FASN (2PX6), it displayed a well-defined binding

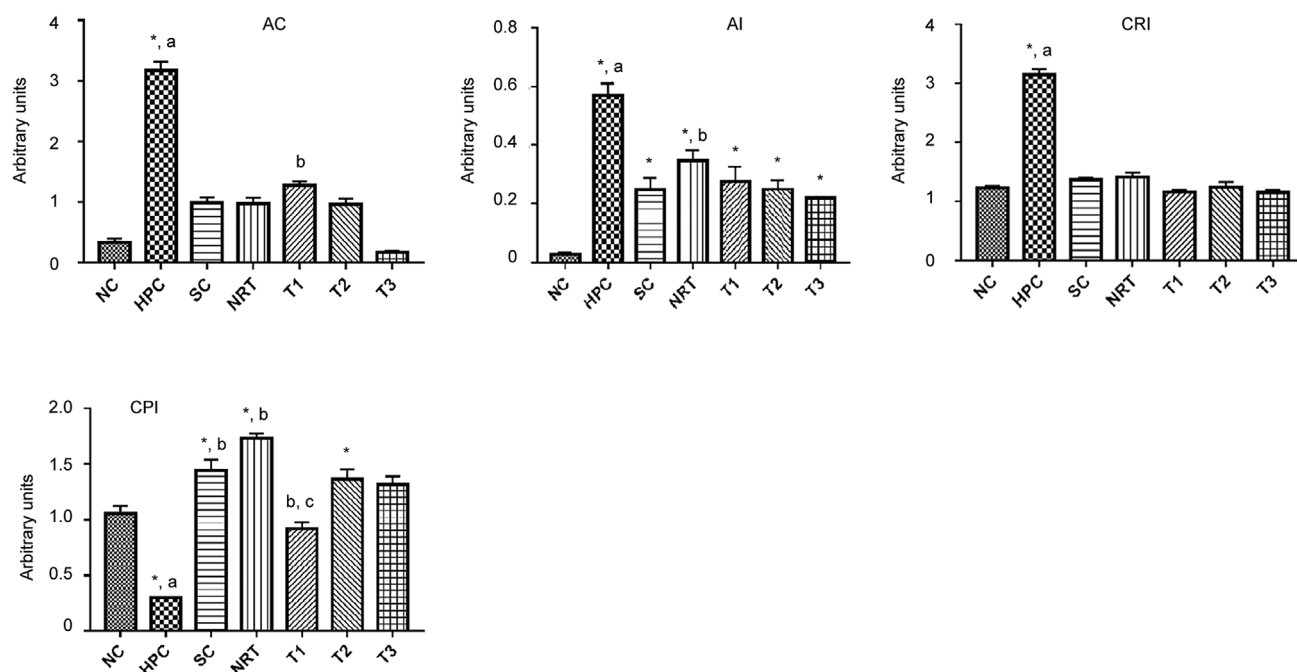


**Fig. 4** Effects of BCE extract on indices of cardiovascular function of hyperlipidemic rats induced by poloxamer 407. \* $p < 0.05$  vs. NC; <sup>a</sup> $p < 0.05$  vs. the treatment groups (SC, NRT, T1, T2, T3); <sup>b</sup> $p < 0.05$  vs. T3. AC, atherogenic coefficient; AI, atherogenic index; BCE, *Buchholzia coriacea*; CRI, coronary risk index; CPI, cardio protective index.

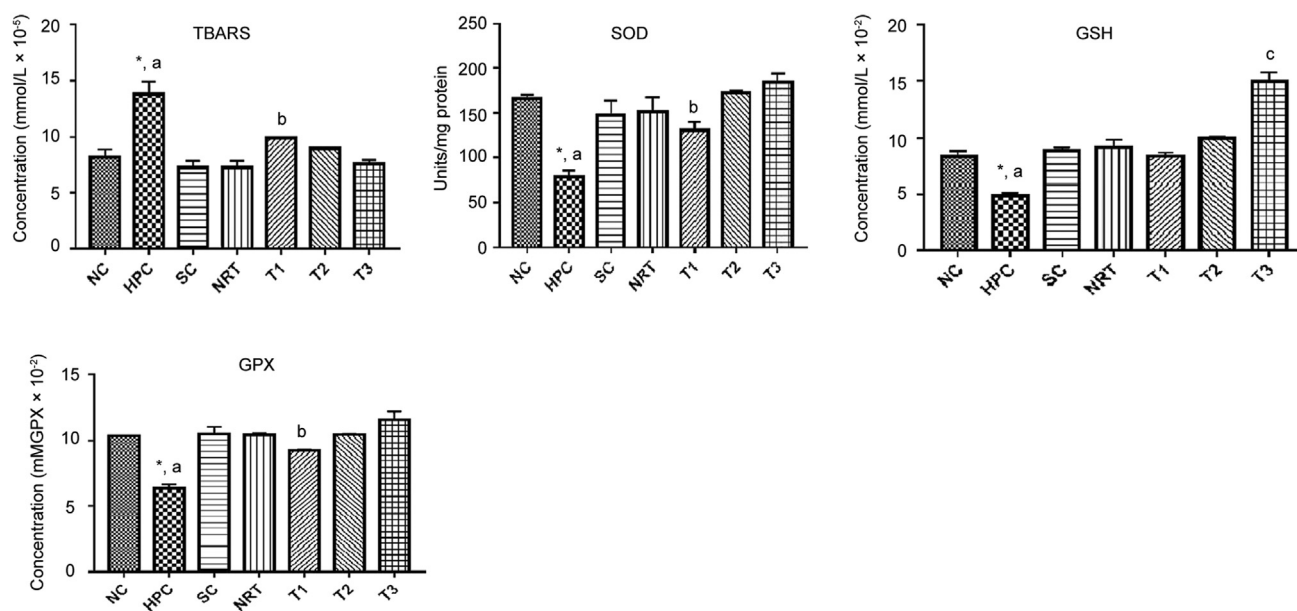


**Fig. 5** Effects of BCE extract on lipid peroxidation and oxidative stress markers of hyperlipidemic rats induced by poloxamer 407. \* $p < 0.05$  vs. NC; <sup>a</sup> $p < 0.05$  vs. the treatment groups (SC, NRT, T1, T2, T3); <sup>b</sup> $p < 0.05$  vs. T3. BCE, *Buchholzia coriacea*; GPX, glutathione peroxidase; GSH, reduced glutathione; TBARS, thiobarbituric acid reactive substances-malondialdehyde; SOD, superoxide dismutase.

pocket constituted of valine, leucine, glutamine, phenylalanine, glycine, isoleucine, and serine residues, where the ligand bound to the core of the pocket with a binding energy of ( $\Delta$ )  $-6.99$  kcal/mol and  $K_i$  of  $11.21$   $\mu$ mol/L. This is indicated in the Supporting Information (**Fig. S1** [available in the online version]). From **Fig. S1** (available in the online version), the significant residues of Pro1817, Val1818, Pro1811, and Leu2130 are attached to the ligand via van der Waals inter-

actions, while residues Lys2137, Glu2133, Tyr2134, Asn2131, Tyr2179, Glu2176, Arg2127, Ile1820, Ile1887, Gln1983, Gln1944, Mse1816, and Asn1815 are bound by alkyl interactions. From **Fig. S1B** (available in the online version), the significant residues of Ile2250, Lys2426, Ser2422, and Gln2374 are attached to the ligand through van der Waals interactions, while residues Phe2375, Ala2419, and Leu2222 are bound by alkyl interactions, and Phe2371 and Phe2423 are bound via



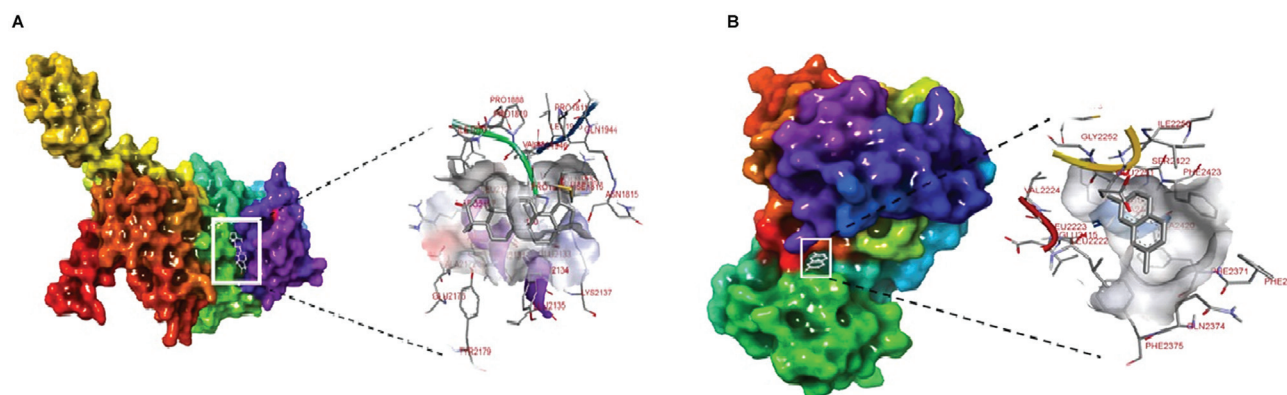


**Fig. 6** Docking structure of different complexes. Analysis of docked pose of (A) acetyl-CoA carboxylase-lupenone complex (1UYS-92158), where the left panel displays the ligand bound at the pocket of the receptor 1UYS and the right panel exhibits the binding pocket residues interacted with the ligand. (B) Fatty acid synthase-2,7-dimethylnaphthalene complex (2PX6-11396), where the left panel displays the ligand bound at the pocket of the receptor 2PX6 and the right panel exhibits the binding pocket residues interacting with the ligand.

Pi–Pi interactions. The post-docking analysis revealed that the optimized lupenone derivative exhibited a higher binding affinity of  $-8.9$  compared with parent lupenone with a binding energy of  $-8.8$ . Moreover, the two-dimensional binding interaction of the optimized derivative, as revealed by discovery studio visualizer 2020, unraveled the presence of hydrogen bond interactions with ACC ( $\rightarrow$  Fig. 51C [available in the online version]), a more stable bond absent in the parent lupenone molecule.

#### ADMET/Pharmacokinetics Predictions of Top-Posed Compounds

The analysis of the lead compounds lupenone (Chem ID: 92158) with its optimized derivative and 2,7-dimethylnaphthalene (Chem ID: 11396) using Lipinski's rule of five, Ghose, and Veber rule is presented in the Supporting Information ( $\rightarrow$  Table S2 [available in the online version]) for its drug-likeness, while the absorption and metabolism profiles of these compounds are presented in the  $\rightarrow$  Tables S3 and S4 (Supporting Information) with the toxicity profile in  $\rightarrow$  Table S5 (Supporting Information). We observed different degrees of violation of the three rules for drug-like properties as indicated. It was only the optimized lupenone derivative that showed high human gastrointestinal tract absorption, while lupenone and 2,7-dimethylnaphthalene exhibited low GIT absorption profiles. These ligands also exhibited varying degrees of cytochrome-P variant inhibition profiles with different toxicological properties toward certain target organs and features.

#### Discussion

In this study, we investigated the potential effect of BCE leaf extracts on hyperlipidemia and oxidative stress indicators in Wistar rats. In addition, we examined the BCE leaf extract as a potential source of ACC and FASN inhibitors and potential hypolipidemic agents *in silico*.

Active ingredients are reportedly implicated in the negative correlation between plant intake and the risk of oxidative stress-related illnesses, including cardiovascular diseases.<sup>31</sup>

This study has identified earlier a significant presence of phytochemicals with an abundance of flavonoids. We detected approximately 44 active ingredients in the plant extract. The significant presence of flavonoids indicates that BCE would be a good source of antioxidants. According to a theory, flavonoids downregulate the expression of NADPH oxidase isoforms, thereby preventing NADPH oxidase from producing superoxide and hence averting oxidative stress.<sup>32</sup> Saponins were also present in the extract in significant amounts, which are highly implicated in lipid metabolism modulation. A proposed mechanism would be that saponins reduce lipid accumulation via autophagy induction.<sup>33</sup>

This study also focused on how BCE affects lipid profiles in HPC rats. P-407 significantly increased TAG, TC, LDL, and VLDL while reducing HDL levels, suggesting sustained hyperlipidemia in the tested animals, which was consistent with previous findings.<sup>34</sup> However, the P-407-induced changing trend in the lipid profiles was significantly reversed upon the BCE leaf extract treatment. This may be due to the presence of saponins in the plant extracts. Saponins reportedly up-regulate acyl-CoA dehydrogenase and carnitine palmitoyltransferase 1, which are involved in oxidation and FASN an ACC downregulation.<sup>35</sup> We observed similar modulatory effects on cardiovascular function indices with positively modulated values such as increased CPI and reduced AC, AI, and CRI.

We also investigated the *in vivo* antioxidant activities of the BCE extract. MDA is one of the consequences of polyunsaturated fatty acid peroxidation in the cells and one of the main markers of lipid peroxidation in oxidative stress, inflammation, and various medical problems; it is thus an important oxidation product. We assessed oxidative stress biomarker levels and observed that the level of TBARS-MDA, an oxidative stress indicator, was significantly higher in the HPC group than in the NC group. However, its reduction was observed in BCE-treated groups, which is assumably caused by the potential of the extract to neutralize hydroxyl and peroxy radicals through antioxidant activities, probably due to the significant presence of flavonoids in the extract.<sup>36</sup>

Moreover, the activities of SOD, GPX, and the concentration of GSH decreased in HPC and similarly increased upon extract administration. Several factors could be responsible for this but the most relevant is potentially the abundant presence of flavonoids in the plant extracts. The antioxidative effect of flavonoids has been documented earlier.<sup>32</sup>

ACC and FASN are two major regulators in fatty acids biosynthesis and fatty acids play several important roles in the body, including their impact as building blocks for phospholipids and glycolipids, target proteins for membranes, an energy-rich fuel source, and fatty acid derivatives, and are used as hormones and intracellular messenger substances.<sup>22</sup> Excessive fat storage could lead to serious health consequences; a condition simply known as hyperlipidemia.<sup>23</sup> Hyperlipidemia cannot be considered a disease in its own right. However, this underlying pathology often leads to serious and ultimately even lethal illnesses. Fatty acids are usually synthesized from acetyl-CoA, a process that requires ATP, biotin, Mg<sup>2+</sup>, and Mn<sup>2+</sup>.<sup>37</sup> The ACC used in this study is the rate-limiting enzyme in fatty acid biosynthesis, while the remaining reactions in fatty acid biosynthesis are executed by a multifunctional protein, fatty acid synthetase (FAS).<sup>38</sup> The ACC (1UYS) and FASN (2PX6) interaction with lupenone and 2,7-dimethyl naphthalene, compounds featuring higher binding poses derived from BCE, have been previously reported to possess hypolipidemic potentials, as documented in earlier studies,<sup>7</sup> which is a validation of the present study.

This study aimed at identifying the best molecule screened from virtual screening of interacting 44 derived chemical compounds via GC-MS (► **Table 2**) with ACC (1UYS) and FASN (2PX6) and comparing their binding potentials to the standard inhibitors of these proteins' essential in fatty acid synthesis. The results were of particular interest as the two compounds lupenone and 2,7-dimethylnaphthalene (► **Fig. 1A, D**) exhibited higher binding affinities compared with standard inhibitors. Lupenone is a triterpenoid<sup>39</sup> and it has a role as a metabolite,<sup>39</sup> deriving from a hydride of lupane while 2,7-dimethylnaphthalene is a dimethylnaphthalene.<sup>40</sup> Triterpenoids, the class of compounds to which lupenone belongs, reportedly exhibit diverse biological activities due to their structural diversity, such as anticarcinogenic, hepatoprotective, antidiabetic, anti-inflammatory, hypolipidemic, antioxidant, and antimicrobial effects,<sup>41</sup> which is in good agreement with the observations of this study.

The detailed drug-like properties of the lead compounds, as revealed by the ADMET properties, are shown in the Supporting Information (► **Table S2**). Some of the results include strong compliance with Lipinski, Ghose, and Vebers rules, with low inhibition of some important drug-metabolizing enzymes (CYP1A2 CYP 2C19, CYP 2D6, CYP 3A4, and CYP 2C9) and low potential organ toxicity (► **Table S3, S4** [Supporting Information]). The ADMET properties of these compounds indicated that they inhibit certain CYP enzymes and might interfere with the metabolism of other drugs. Their other drug-able properties and ADMET properties are shown in supplementary data (► **Tables S3–S5** [Supporting Information]). Overall, the ADMET properties of these compounds

indicated that the optimized lupenone derivate and 2,7-dimethylnaphthalene had better octanol-water coefficient and better gastrointestinal tract permeability presenting these compounds as potential drug candidates. More so, the toxicity profile of these compounds showed they are relatively non-toxic to vital organs.

Therefore, this study presents lupenone and 2,7-dimethylnaphthalene, as two novel BCE-derived hypolipidemic compounds, as potential agents that take their effect via their stronger binding potentials to ACC and FASN in docking. This study thus provided potential therapeutic drug candidates for the research efforts to treat hyperlipidemia and its associated disease complications, especially since these compounds showed higher affinity for the studied proteins *in silico* than established standard inhibitors of the proteins firsocostat and C75 *trans*. One of the possible effector mechanisms of these potential drug agents against ACC and FASN could be based on the premise that lupenone and 2,7-dimethylnaphthalene inhibit ACC and FASN activities by interacting within the phosphopeptide-acceptor of bonded amino acids and dimerization site of these enzymes to prevent their dimerization,<sup>42</sup> since the enzymes are only active in a dimerized form. This interaction is exemplified by the structure of lupenone and 2,7-dimethylnaphthalene, modeled into the crystal structure of the protein complexes.

## Conclusion

To the best of our knowledge, this study was the first to reveal that BCE is a potential source of hypolipidemic agents and presented two new potential hypolipidemic BCE agents, lupenone and 2,7-dimethylnaphthalene, with potential usefulness in dyslipidemia management via ACC and FASN inhibition from natural plant sources. Moreover, these compounds also exhibited promising druggable properties *in silico*. However, further preclinical, and clinical wet laboratory procedures would be required to validate these outcomes in future studies.

### Ethics Approval and Consent to Participate

The Convention on Trade in Endangered Species of Wild Fauna and Flora was complied with by this study. Additionally, the Federal University of Health Sciences, Otukpo, Nigeria and the Department of Biochemistry Ethical Committee on Research, Innovation, and Institutional Ethical Committee authorized the study (-FUHSO/ET/BCH/22/002).

### Supporting Information

Chemical profile of methanolic BCE (► **Table S1** [Supporting Information]), the drug-likeness, absorption profile, metabolism, and toxicity profiles of the top-posed compounds (► **Tables S2–S5** [Supporting Information]), as well as a two-dimensional representation of the molecular interactions between protein and ligand (► **Fig. S1** [Supporting Information]) are included in the Supporting Information (available in the online version).

**Conflict of Interest**

None declared.

**Acknowledgments**

The authors thank Mr. Anaga Charles, Senior Laboratory Technologist at Evangel University Akaeze, who was involved in the extraction of the leaves helped, and AA Ibitoye, who performed the GC-MS analysis of the plant extract.

**References**

- Oteng Mintah S, Asafo-Agyei T, Archer MA, et al. Medicinal plants for treatment of prevalent diseases. In: Perveen S, Al-Taweel A. Pharmacognosy - Medicinal Plants. 2019 ed. London: IntechOpen
- Hedayatnia M, Asadi Z, Zare-Feyzabadi R, et al. Dyslipidemia and cardiovascular disease risk among the MASHAD study population. *Lipids Health Dis* 2020;19(01):42
- Carson JAS, Lichtenstein AH, Anderson CAM, et al; American Heart Association Nutrition Committee of the Council on Lifestyle and Cardiometabolic Health; Council on Arteriosclerosis, Thrombosis and Vascular Biology; Council on Cardiovascular and Stroke Nursing; Council on Clinical Cardiology; Council on Peripheral Vascular Disease; and Stroke Council. Dietary cholesterol and cardiovascular risk: a science advisory from the American Heart Association. *Circulation* 2020;141(03):e39–e53
- Chen L, Duan Y, Wei H, et al. Acetyl-CoA carboxylase. (ACC) as a therapeutic target for metabolic syndrome and recent developments in ACC1/2 inhibitors. *Expert Opin Investig Drugs* 2019;28(10):917–930
- Chen FJ, Yin Y, Chua BT, Li P. CIDE family proteins control lipid homeostasis and the development of metabolic diseases. *Traffic* 2020;21(01):94–105
- Fhu CW, Ali A. Fatty acid synthase: an emerging target in cancer. *Molecules* 2020;25(17):3935
- Omayone TP, Salami AT, Odukanmi AO, Olaleye SB. Diet containing seeds of *Buchholzia coriacea* accelerates healing of acetic acid induced colitis in rats. *Asian Pac J Trop Biomed* 2018;8(03):166–172
- Onasanwo SA, Obembe OO, Faborode SO, Elufioye TO, Adisa RA. Neuro-pharmacological potentials of *Buchholzia coriacea* (Engl.) seeds in laboratory rodents. *Afr J Med Med Sci* 2013;42(02):131–142
- Zhang QW, Lin LG, Ye WC. Techniques for extraction and isolation of natural products: a comprehensive review. *Chin Med* 2018;13:20
- Udeozor PA, Ibiama UA, Uti DE, et al. Antioxidant and anti-anemic effects of ethanol leaf extracts of *Mucuna poggei* and *Telfairia occidentalis* in phenyl-hydrazine-induced anemia in wistar albino rats. *Ibnosina J Med Biomed Sci* 2022;14(03):116–126
- Sofowara A. Medicinal Plants and Traditional Medicine in Africa. Ibadan: Spectrum Books Ltd.; 1993:191–289
- Evans WC, Evans D, Trease GE. Trease and Evans' Pharmacognosy. 15th ed. Edinburgh: WB Saunders; 2002:215
- De S, Dey YN, Ghosh AK. Phytochemical investigation and chromatographic valuation of the different extracts of tuber of *amorphophalluspaeoniifolius* (araceae). *Int J Res Pharm Biomed Sci* 2010;1(05):150–157
- Uti DE, Atangwho IJ, Eyong EU, et al. African walnuts (*Tetracarpidium conophorum*) modulate hepatic lipid accumulation in obesity via reciprocal actions on HMG-CoA reductase and para-oxonase. *Endocr Metab Immune Disord Drug Targets* 2020;20(03):365–379
- Chaudhary HR, Brocks DR. The single dose poloxamer 407 model of hyperlipidemia; systemic effects on lipids assessed using pharmacokinetic methods, and its effects on adipokines. *J Pharm Pharm Sci* 2013;16(01):65–73
- Alum EU, Ibiama UA, Emmanuel I, et al. Antioxidant effect of *Buchholzia coriacea* ethanol leaf extract and fractions on Freund's adjuvant-induced arthritis in albino rats: a comparative study. *Slov Vet Res* 2022;59(01):31–45
- Igharo OG, Akinfenwa Y, Isara AR, et al. Lipid profile and atherogenic indices in nigerians occupationally exposed to e-waste: a cardiovascular risk assessment study. *Maedica (Buchar)* 2020;15(02):196–205
- Heber MF, Ferreira SR, Vélez LM, Motta AB. Prenatal hyperandrogenism and lipid profile during different age stages: an experimental study. *Fertil Steril* 2013;99(02):551–557
- Warnick GR, Albers JJ. A comprehensive evaluation of the heparin-manganese precipitation procedure for estimating high density lipoprotein cholesterol. *J Lipid Res* 1978;19(01):65–76
- Friedewald WT, Levy RI, Fredrickson DS. Estimation of the concentration of low-density lipoprotein cholesterol in plasma, without use of the preparative ultracentrifuge. *Clin Chem* 1972;18(06):499–502
- Ogar I, Egbung GE, Nna VU, Atangwho IJ, Itam EH. Hyptis verticillata attenuates dyslipidaemia, oxidative stress and hepato-renal damage in streptozotocin-induced diabetic rats. *Life Sci* 2019;219:283–293
- Buege JA, Aust SD. Microsomal lipid peroxidation. *Methods Enzymol* 1978;52:302–310
- Li X. Improved pyrogallol autoxidation method: a reliable and cheap superoxide-scavenging assay suitable for all antioxidants. *J Agric Food Chem* 2012;60(25):6418–6424
- Ellman GL. Tissue sulphhydryl groups. *Arch Biochem Biophys* 1959;82(01):70–77
- Hu ML. Measurement of protein thiol groups and glutathione in plasma. *Methods Enzymol* 1994;233:380–385
- Dallakyan S, Olson AJ. Small-molecule library screening by docking with PyRx. *Methods Mol Biol* 2015;1263:243–250
- Trott O, Olson AJ. AutoDock Vina: improving the speed and accuracy of docking with a new scoring function, efficient optimization, and multithreading. *J Comput Chem* 2010;31(02):455–461
- Butnariu M, Sarac I, Coltescu Ar. The importance of solubility for new drug molecules. *Biomed Pharmacol J* 2020;13(02):577–583
- Yang H, Sun L, Wang Z, Li W, Liu G, Tang Y. ADMETopt: a web server for ADMET optimization in drug design via scaffold hopping. *J Chem Inf Model* 2018;58(10):2051–2056
- Daina A, Michielin O, Zoete V. SwissADME: a free web tool to evaluate pharmacokinetics, drug-likeness and medicinal chemistry friendliness of small molecules. *Sci Rep* 2017;7:42717
- Tang GY, Meng X, Li Y, Zhao CN, Liu Q, Li HB. Effects of vegetables on cardiovascular diseases and related mechanisms. *Nutrients* 2017;9(08):857
- Jubaidi FF, Zainalabidin S, Taib IS, Hamid ZA, Budin SB. The potential role of flavonoids in ameliorating diabetic cardiomyopathy via alleviation of cardiac oxidative stress, inflammation and apoptosis. *Int J Mol Sci* 2021;22(10):5094
- Bai J, Zhu Y, He L, et al. Saponins from bitter melon reduce lipid accumulation via induction of autophagy in *C. elegans* and HepG2 cell line. *Curr Res Food Sci* 2022;5:1167–1175
- Murphy SA, Cannon CP, Wiviott SD, et al. Effect of intensive lipid-lowering therapy on mortality after acute coronary syndrome (a patient-level analysis of the Aggrastat to Zocor and Pravastatin or Atorvastatin Evaluation and Infection Therapy-Thrombolysis in Myocardial Infarction 22 trials). *Am J Cardiol* 2007;100(07):1047–1051
- Pérez-Ramírez IF, González-Dávalos ML, Mora O, et al. Cardiac lipid metabolism is modulated by *Casimiroa edulis* and *Crataegus pubescens* aqueous extracts in high fat and fructose (HFF) diet-fed obese rats. *Eur J Lipid Sci Technol* 2019;121:1900157
- Gheith I, El-Mahmoudy A. Laboratory evidence for the hemato-poietic potential of *Beta vulgaris* leaf and stalk extract in a phenylhydrazine model of anemia. *Braz J Med Biol Res* 2018;51(11):e7722

- 37 Larry RE. Hyperlipidemias. In: Engelking L, ed. Textbook of Veterinary Physiological Chemistry. 3rd ed. Cambridge: Academic Press; 2015:427–433
- 38 Engelking LR. Chapter 56 - Fatty acid biosynthesis. In: Engelking LR. 3rd ed. Textbook of Veterinary Physiological Chemistry. Boston: Academic Press.; 2015:358–364
- 39 Xu F, Yang L, Huang X, Liang Y, Wang X, Wu H. Lupenone is a good anti-inflammatory compound based on the network pharmacology. *Mol Divers* 2020;24(01):21–30
- 40 Davies A, Warren KD. Nitration of dimethylnaphthalenes in acetic anhydride. *J Chem Soc B* 1969:873–878
- 41 Sandeep GS. Chapter 12 - Triterpenoids: structural diversity, biosynthetic pathway, and bioactivity. *Studies in Natural Products Chemistry* 2020;67:411–461
- 42 Harriman G, Greenwood J, Bhat S, et al. Acetyl-CoA carboxylase inhibition by ND-630 reduces hepatic steatosis, improves insulin sensitivity, and modulates dyslipidemia in rats. *Proc Natl Acad Sci U S A* 2016;113(13):E1796–E1805